A Covalent Vanadium(III) 2-Dimensional Network and Vanadyl Chains Linked by Aryldioxides

Joseph M. Tanski and Peter T. Wolczanski*

Baker Laboratory, Department of Chemistry & Chemical Biology, Cornell University, Ithaca, New York 14853

Received July 11, 2000

Thermolysis of (^{i}PrO)$_4$V and 2,6-dihydroxynaphthalene in 4-(3-phenylpropyl)pyridine afforded [*mer*-V($\mu_{2,6}$-$OC_{10}H_6O)_{1.5}$(4-(3-phenylpropyl)py)$_3$]$_n$ (**1**; $C_{57}H_{54}N_3O_3V$, triclinic, $P\bar{1}$, a = 10.450(2) Å, b = 14.098(3) Å, c = 16.765(3) Å, α = 100.09(3)°, β = 103.85(3)°, γ = 103.08(3)°, Z = 2) and oxidation product bis-2,6-dinaphthol. Paramagnetic (S = 1) **1** adopts a bricklike motif of aryldioxide-connected V(III) centers whose channels are filled with the bound 4-(3-phenylpropyl)py. A similar procedure involving (^{i}PrO)$_3$VO provided the linear chain [($\mu_{2,6}$-$OC_{10}H_6O$)(4-(3-phenylpropyl)py)$_2$VO]$_n$ (**2**; $C_{38}H_{36}N_2O_3V$, monoclinic, $P2_1/c$, a = 10.6172(2) Å, b = 9.4477(3) Å, c = 31.8129(8) Å, β = 95.20(3)°, Z = 4). Interchain pyridine ring-edge to phenyl-face interactions generate a sheet of like-oriented oxos, but adjacent sheets are oriented in opposition so that no net dipole exists. Another 1-dimensional chain, [($\mu_{1,4}$-OC_6H_4O)(py)$_2$VO]$_n$ (**3**; $C_{16}H_{14}N_2O_3V$, monoclinic, $P2_1/c$, a = 8.377(2) Å, b = 16.675(3) Å, c = 11.061(2) Å, β = 103.91(3)°, Z = 4), was prepared by heating (^{i}PrO)$_4$V and hydroquinone in pyridine. Pyridines of adjacent chains interpenetrate to form a sheet, but oxos in adjacent chains are now in opposition.

Introduction

Initial investigations of covalent metal−organic networks (CMONs), synthesized from early-transition-metal alkoxide and dihydroxyaromatic (DHA) precursors, led to an understanding of the elements that control dimensionality. In the absence of Lewis bases, titanium dialkoxyaromatic compounds tend to form 3-dimensional body-centered (e.g., [$Ti_2(\mu_{1,4}$-$OC_6H_4O)_2(\mu_{1,4}$-$OC_6H_4OH)_2(\mu$-$OC_6H_4OH)_2]_\infty$,[1,2] [$Ti_2(\mu_{2,7}$-$OC_{10}H_6O)_2(\mu_{2,7}$:η^2,η^1-$OC_{10}H_6OH)_2(O^iPr)_2]_\infty$),[2] hexagonal (e.g., [$Ti_2(\mu_{1,4}$-$OC_6H_4O)_2$-($\mu_{1,4}$:$\eta^2$,$\eta^1$-$OC_6H_4O)_2(OH_2)_2\cdot(H_2O)_2\cdot(HOC_6H_4OH)\cdot$(Me-CN)]$_\infty$),[2] or primitive (e.g., {[Ti(μ:η^2,η^1-4,4′-$OC_{12}H_8O)_{0.5}$(μ-4,4′-$OC_{12}H_8O$)(O^iPr)(HO^iPr)]$_2\cdot$THF}$_n$)[3] secondary structural motifs based on $Ti_2(\mu$-OAr)$_2$ building blocks. There can be exceptions, such as {[Ti($\mu_{1,3}$-OC_6H_4O)(μ-1,3-OC_6H_4OH)(1,3-OC_6H_4OH)-(HO^iPr)]$_2$}$_n$,[3] whose 2-dimensional network arises from the restricted linking ability of the μ-1,3-OC_6H_4O spacer derived from resorcinol. In the presence of pyridine donors (L), 2-dimensional networks abound because the linking capacity of typical (μ-OArO)$_4$TiL$_2$ mononuclear building blocks is best realized through flat (*trans*) or rippled (*cis*) sheets.[1,4]

Previously, emphasis was placed on differentiating the strictly covalent nature of the bonding in CMONs[1−4] in comparison to the dative interactions that dominate the construction of these new coordination polymers.[5] In an attempt to develop CMON species that exhibit intermetallic communication, systems containing d^n (n > 0) metal centers were sought.[6,7] Given the precedent set in 2-dimensional titanium(IV) CMONs, analogous V(IV) counterparts, and their solid solutions,[4] it seemed prudent to continue evaluation of vanadium. During the course of examining (^{i}PrO)$_3$VO and (^{i}PrO)$_4$V[8] as potential precursors to vanadium-based CMONs, the trend toward a reduction in dimensionality in the presence of donors was reinforced. In addition to 2-dimensional species, 1-dimensional compounds have been produced, and the compositions of both were unexpected because the well-known oxidative coupling chem-

(1) Vaid, T. P.; Lobkovsky, E. B.; Wolczanski, P. T. *J. Am. Chem. Soc.* **1997**, *119*, 8742−8743.
(2) Vaid, T. P.; Tanski, J. M.; Pette, J. M.; Lobkovsky, E. B.; Wolczanski, P. T. *Inorg. Chem.* **1999**, *38*, 3394−3405.
(3) Tanski, J. M.; Lobkovsky, E. B.; Wolczanski, P. T. *J. Solid State Chem.* **2000**, *152*, 130−140.
(4) Tanski, J. M.; Vaid, T. P.; Lobkovsky, E. B.; Wolczanski, P. T. *Inorg. Chem.* **2000**, *39*, 4756−4765.
(5) For some recent coordination polymers based on dative interactions, see: (a) O'Keeffe, M.; Eddaoudi, M.; Li, H.; Reineke, T.; Yaghi, O. M. *J. Solid State Chem.* **2000**, *152*, 3−20. (b) Batten, S. R.; Robson, R. *Angew. Chem., Int. Ed. Engl.* **1998**, *37*, 1460−1494. (c) Reineke, T. M.; Eddaoudi, M.; Moler, D.; O'Keeffe, M.; Yaghi, O. M. *J. Am. Chem. Soc.* **2000**, *122*, 4843−4844. (d) Michelsen, U.; Hunter, C. A. *Angew. Chem., Int. Ed. Engl.* **2000**, *39*, 764−767. (e) Pan, L.; Huang, X.; Li, J.; Wu, Y.; Zheng, N. *Angew. Chem., Int. Ed. Engl.* **2000**, *39*, 527−530. (f) Diskin-Posner, Y.; Dahal, S.; Goldberg, I. *Angew. Chem., Int. Ed. Engl.* **2000**, *39*, 1288−1292. (g) Carlucci, L.; Ciani, G.; Moret, M.; Proserpio, D. M.; Rizzato, S. *Angew. Chem., Int. Ed. Engl.* **2000**, *39*, 1506−1510. (h) Carlucci, L.; Ciani, G.; Proserpio, D. M. *J. Chem. Soc., Chem. Commun.* **1999**, 449−450. (i) Keller, S. W.; Lopez, S. *J. Am. Chem. Soc.* **1999**, *121*, 6306−6307. (j) Power, K. N.; Hennigar, T. L.; Zaworotko, M. J. *J. Chem. Soc., Chem. Commun.* **1998**, 595−596. (k) Kepert, C. J.; Rosseinsky, M. J. *J. Chem. Soc., Chem. Commun.* **1999**, 375−376. (l) Hirsch, K. A.; Wilson, S. R.; Moore, J. S. *Inorg. Chem.* **1997**, *36*, 2960−2968. (m) Chang, H.-C.; Ishii, T.; Kondo, M.; Kitagawa, S. *J. Chem. Soc., Dalton Trans.* **1999**, 2467−2476.
(6) *Inorganic Materials*; Bruce, D. W., O'Hare, D., Eds.; John Wiley & Sons: New York, 1992.
(7) For some recent coordination polymers manifesting some intermetallic communication, see: (a) Barandika, M. G.; Hernandez-Pino, L.; Urtiaga, M. K. Cortes, R.; Lezama, L.; Arriortua, I.; Rojo, T. *J. Chem. Soc., Dalton Trans.* **2000**, 1469−1473. (b) Montserrat, M.; Resino, I.; Ribas, j.; Stoeckli-Evans, H. *Angew. Chem., Int. Ed. Engl.* **2000**, *39*, 191−193. (c) Larionova, J.; Kahn, O.; Gohlen, S. Lahcene, O.; Clerac, R. *J. Am. Chem. Soc.* **1999**, *121*, 3349−3356. (d) Manson, J. L.; Incarvito, C. D.; Rheingold, A. L.; Miller, J. S. *J. Chem. Soc., Dalton Trans.* **1998**, 3705−3706. (e) Lloret, F.; De Munno, G.; Julve, M.; Cano, J.; Ruiz, R.; Caneschi, A. *Angew. Chem., Int. Ed. Engl.* **1998**, *37*, 135−138.
(8) Bradley, D. C.; Mehta, M. L. *Can. J. Chem.* **1962**, *40*, 1183−1188.

10.1021/ic000756z CCC: $20.00
Published on Web 12/07/2000

istry of 2,6-dihydroxynaphthalene[9] interfered with the anticipated network formation. Herein are reported d^1 and d^2 CMON materials derived from in situ reduction of the vanadium precursors.

Results

2-Dimensional [*mer*-V($\mu_{2,6}$-$OC_{10}H_6O$)$_{1.5}$(4-(3-phenylpropyl)-py)$_3$]$_n$ (1). 1. Synthesis. An immediate blackening of the solution was observed when (^{i}PrO)$_4$V[8] and excess 2,6-dihydroxynaphthalene were mixed in 4-(3-phenylpropyl)pyridine. Thermolysis of the mixture at 100 °C afforded small crystals after a few days, and larger crystals of orange [*mer*-V($\mu_{2,6}$-$OC_{10}H_6O$)$_{1.5}$(4-(3-phenylpropyl)py)$_3$]$_n$ (**1**) were harvested after 35 d (eq 1).

$$(^i\mathrm{PrO})_4\mathrm{V} + 2.5\mathrm{HOC_{10}H_6OH} \xrightarrow[100\ ^\circ\mathrm{C}]{\text{4-(3-phenylpropyl)py}} 4\,^i\mathrm{PrOH} + 0.5(2,6\text{-}(\mathrm{HO})_2\mathrm{C_{10}H_5})_2 + [\text{mer-V}(\mu_{2,6}\text{-}\mathrm{OC_{10}H_6O})_{1.5}(\text{4-(3-phenylpropyl)py})_3]_n\ (\mathbf{1}) \quad (1)$$

Extraction of the filtrate from a preparation of [*mer*-V($\mu_{2,6}$-$OC_{10}H_6O$)$_{1.5}$(4-(3-phenylpropyl)py)$_3$]$_n$ (**1**) revealed the coupled product bis-2,6-dinaphthol ((2,6-(HO)$_2$C$_{10}$H$_5$)$_2$), which was identified by ^{1}H NMR spectroscopy and thin-layer chromatography through comparison with an authentic sample. According to standard oxidative coupling procedures,[9] treatment of 2,6-dihydroxynaphthalene with $FeCl_3 \cdot 3H_2O$ in MeCN/H_2O at 23 °C for 1.5 h afforded bis-2,6-dinaphthol in <5% yield (eq 2)

$$2\mathrm{HOC_{10}H_6OH} + 2\mathrm{FeCl_3 \cdot 3H_2O} \xrightarrow[23\ ^\circ\mathrm{C}]{\mathrm{MeCN/H_2O}} (2,6\text{-}(\mathrm{HO})_2\mathrm{C_{10}H_5})_2 + 2\mathrm{FeCl_2} + 2\mathrm{HCl} \quad (2)$$

upon crystallization from 60:40 EtOAc/hexane following chromatography on silica gel. The low yield (unoptimized) of the coupling is due to the reactivity of the bis-2,6-dinaphthol toward additional oxidative couplings, leading to the formation of oligomeric byproducts.

2. X-ray Crystal Structure. Crystals of [*mer*-V($\mu_{2,6}$-$OC_{10}H_6O$)$_{1.5}$(4-(3-phenylpropyl)py)$_3$]$_n$ (**1**) were very weakly diffracting, necessitating the use of synchrotron radiation at the Cornell High Energy Synchrotron Source (CHESS; Table 1). The structure of **1** is a 2-dimensional (6,3) net whose T-connections derived from the *mer* octahedral coordination (Figure 1) of the $\mu_{2,6}$-$OC_{10}H_6O$ spacers comprise a brick-wall-type motif. Figure 2 illustrates a single sheet of the material that is shown with and without some of the 4-(3-phenylpropyl)pyridines.

The VO_3N_3 core of [*mer*-V($\mu_{2,6}$-$OC_{10}H_6O$)$_{1.5}$(4-(3-phenylpropyl)py)$_3$]$_n$ (**1**) is roughly octahedral and has a *mer* arrangement with normal V−O and V−N bond lengths (Table 2, Figure 1). The V−O2 bond opposite the 4-(3-phenylpropyl)pyridine is slightly shorter (1.902(3) Å) than the aryloxide bonds that oppose one another (d(V−O1) = 1.910(3) Å, d(V−O3) = 1.914(3) Å). The reverse is true for the 4-(3-phenylpropyl)-pyridine ligands; the V−N3 bond opposite the aryoxide is long (2.264(4) Å) compared to those of the *trans*-pyridines (d(V−N2) = 2.156(4) Å, d(V−N1) = 2.170(4) Å). On the basis of the higher *trans* influence of aryloxides vs pyridine ligands, this is expected. Since the 4-(3-phenylpropyl)pyridines are more sterically influential at the core than the naphthoxides, whose bulk initiates two bond lengths from the vanadium, deviation from strict octahedral geometry was expected to be greater for the former. Curiously, the ∠(O1−V−O3) of 167.4(2)° is less than the N1−V−N2 angle of 174.4(2)°, and the accompanying O1−V−O2 and O2−V−O3 angles of 99.4(2)° and 93.0(2)°, respectively, are greater than the corresponding N2−V−N3 and N1−V−N3 angles of 94.7(2)° and 90.4(2)°, respectively. In C_{2v} symmetry, the "t_{2g}" set of orbitals splits into b_1 (d_{xz}, O_3VN plane), a_2 (d_{xy}), and b_2 (d_{yz}) components; hence, no formal Jahn−Teller distortions are appropriate to rationalize the subtle distortions for this $S = 1$ (vide infra) center, whose orbital ordering is likely to be $d_{yz}^1 d_{xy}^1 d_{xz}^0$ ($b_2^1 a_2^1 \rightarrow {}^3B_1$). Some mimimal angular deviations from 90° may be needed to maximize the π-donation of the aryloxides and perhaps some weak π-accepting interactions of the pyridines. π-Interactions of this type can cause pronounced distortions in 5-coordination,[10] and subtler variations may be expected in 6-coordination.

The three 4-(3-phenylpropyl)pyridines per metal center fill void space (Figure 2) and buttress neighboring layers without any obvious parallel or 90° π-stacking interactions.[11,12] Neigh-

Table 1. X-ray Crystallographic Data on 1- and 2-Dimensional Vanadium Compounds (Crystal Data, Data Collection and Refinement)

	1	**2**	**3**
empirical formula	$C_{57}H_{54}N_3O_3V$	$C_{38}H_{36}N_2O_3V$	$C_{16}H_{14}N_2O_3V$
fw	879.97	619.13	333.23
space group	$P\bar{1}$	$P2_1/c$	$P2_1/c$
Z	2	4	4
a, Å	10.450(2)	10.6172(2)	8.377(2)
b, Å	14.098(3)	9.4477(3)	16.675(3)
c, Å	16.765(3)	31.8129(8)	11.061(2)
α, deg	100.09(3)	90	90
β, deg	103.85(3)	95.20(3)	103.91(3)
γ, deg	103.08(3)	90	90
V, Å^3	2266.1(8)	3177.95(4)	1499.8(5)
D_{calcd}, g·cm^{-3}	1.290	1.295	1.476
abs coeff, mm^{-1}	0.269	0.352	0.675
temp, K	108(2)	173	165
radiation (λ, Å)	0.980 80	0.710 73	0.710 73
GOF[a] on F^2	1.703	1.425	1.055
R^b indices	R1 = 0.0608	R1 = 0.0798	R1 = 0.0407
[$I > 2\sigma(I)$]	wR2 = 0.1961	wR2 = 0.2084	wR2 = 0.0714
R^b indices	R1 = 0.0688	R1 = 0.1272	R1 = 0.1714
(all data)	wR2 = 0.2029	wR2 = 0.2377	wR2 = 0.1435

[a] GOF = $[\sum w(|F_o| - |F_c|)^2/(n-p)]^{1/2}$, n = number of independent reflections, p = number of parameters. [b] R1 = $\sum||F_o| - |F_c||/\sum|F_o|$; wR2 = $[\sum w(|F_o| - |F_c|)^2/\sum wF_o^2]^{1/2}$.

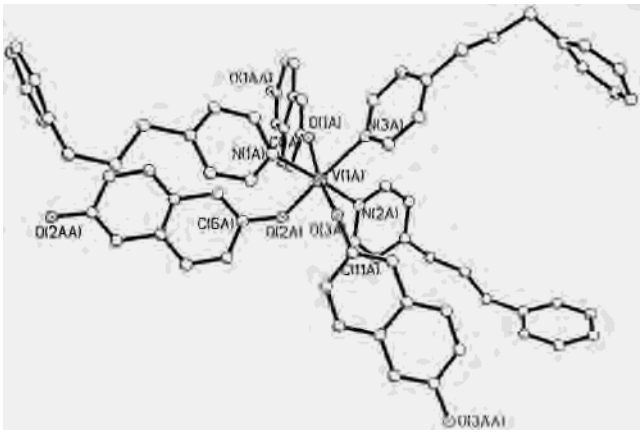

Figure 1. *mer* octahedral VO_3N_3 core of [*mer*-V($\mu_{2,6}$-$OC_{10}H_6O$)$_{1.5}$(4-(3-phenylpropyl)py)$_3$]$_n$ (**1**).

(9) Dewar, M. J. S.; Nakaya, T. *J. Am. Chem. Soc.* **1968**, *90*, 7134−7135.

(10) Ward, T. R.; Bürgi, H.-B.; Gilardoni, F.; Weber, J. *J. Am. Chem. Soc.* **1997**, *119*, 11974−11985.

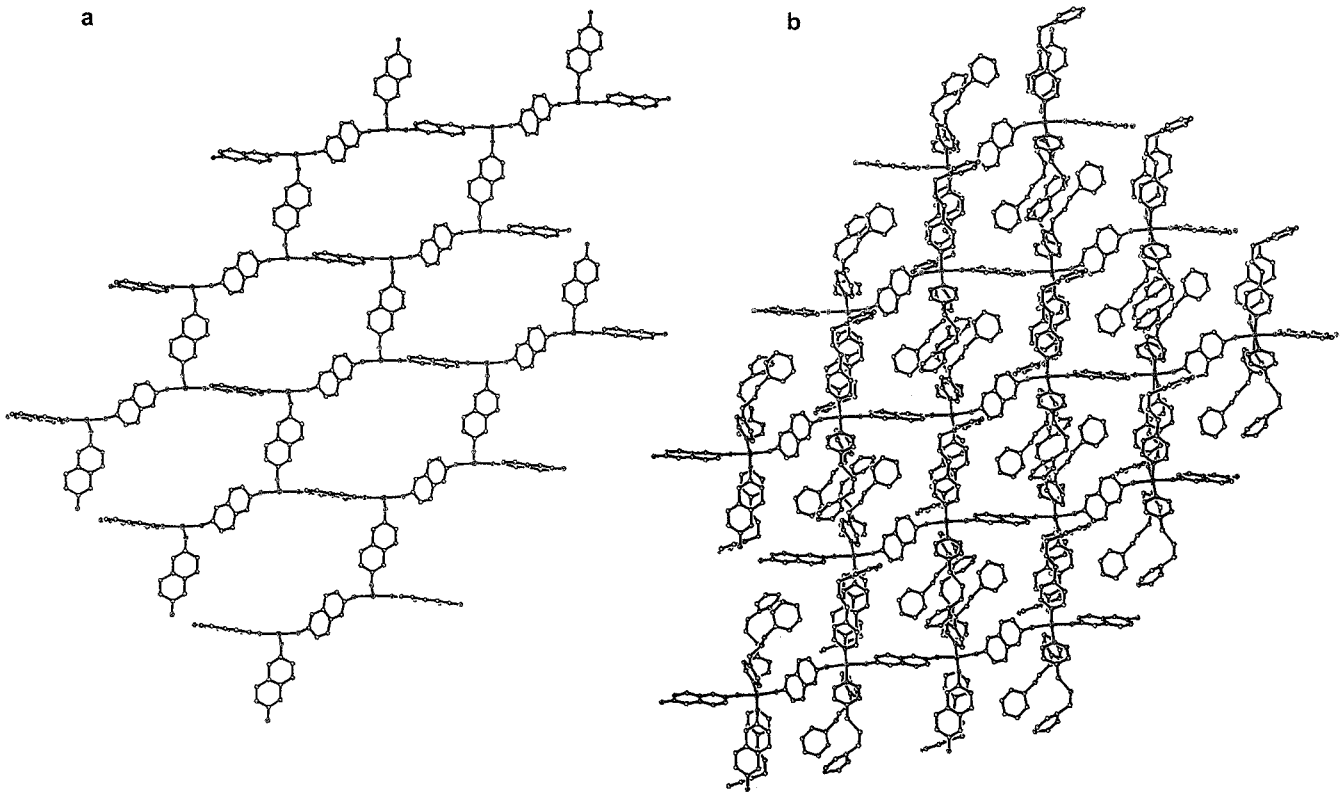

Figure 2. Empty (a; 4-(3-phenylpropyl)pyridines removed) and filled (b) pseudobrick motif of [*mer*-V($\mu_{2,6}$-$OC_{10}H_6O$)$_{1.5}$(4-(3-phenylpropyl)py)$_3$]$_n$ (**1**).

Table 2. Selected Interatomic Distances (Å) and Angles (deg) in [*mer*-V($\mu_{2,6}$-$OC_{10}H_6O$)$_{1.5}$(4-(3-phenylpropyl)py)$_3$]$_n$ (**1**)

V−O1	1.910(3)	V−N1	2.170(4)	O1−C1	1.359(6)
V−O2	1.902(3)	V−N2	2.156(4)	O2−C6	1.356(6)
V−O3	1.914(3)	V−N3	2.264(4)	O3−C11	1.345(6)
O1−V−O3	167.36(14)	N1−V−N2	174.41(14)	N1−V−O1	87.57(15)
O1−V−O1	99.38(14)	N1−V−N3	90.39(14)	N2−V−O1	90.74(15)
O2−V−O3	92.95(14)	N2−V−N3	94.72(15)	N3−V−O1	83.75(15)
N1−V−O2	89.95(14)	N1−V−O3	89.72(14)	V−O1−C1	136.5(3)
N2−V−O2	85.08(17)	N2−V−O3	93.06(14)	V−O2−C6	133.2(3)
N3−V−O2	176.86(14)	N3−V−O3	83.92(15)	V−O3−C11	131.3(3)

boring layers of [*mer*-V($\mu_{2,6}$-$OC_{10}H_6O$)$_{1.5}$(4-(3-phenylpropyl)-py)$_3$]$_n$ (**1**) are slightly offset from one another (21.3°), with d(V···V) = 10.4 Å, and the channels described by the distorted (6,3) "bricks" of each sheet are filled with two 4-(3-phenylpropyl)-pyridines, the unique one (N3) and another (N2). The third 4-(3-phenylpropyl)pyridine (N1) is aligned with the unique aryloxide (O2), and helps buttress the layers. The (6,3) connections deviate from a true rectangular brick pattern in that the V−V transannular distance is ∼14.4 Å compared to each $\mu_{2,6}$-$OC_{10}H_6O$ connected V−V distance of ∼10.6 Å (Figure 3). This discrepancy is far too large to be attributed to core distortions, and arises from the 2,7-dialkoxynaphthalene, which enforces a subtle boatlike configuration to each ring, rendering the sheets slightly rippled.

The powder diffraction pattern of [*mer*-V($\mu_{2,6}$-$OC_{10}H_6O$)$_{1.5}$-(4-(3-phenylpropyl)py)$_3$]$_n$ (**1**) calculated from the single-crystal data was not always comparable to that of the bulk sample, and depended on how the latter was originally collected from the reaction mixture. Some of the 4-(3-phenylpropyl)pyridine may be washed out or displaced via rinsing with THF, and samples degraded in CD_3OD and analyzed by ^{1}H NMR spectroscopy revealed 2,6-dihydroxynaphthalene:4-(3-phenylpropyl)pyridine ratios that were higher than the 1:2 expected from the single-crystal data. By light microscopy, all of the material appeared as orange crystals of the same shape and size regardless of the workup procedure. It is speculated that some collapse of the lattice may occur upon loss of 4-(3-phenylpropyl)pyridine during washing or drying of the crystals, and this is reflected in the powder XRD analysis.

3. Magnetic and Chemical Properties. Magnetic susceptibility measurements were conducted on [*mer*-V($\mu_{2,6}$-$OC_{10}H_6O$)$_{1.5}$-(4-(3-phenylpropyl)py)$_3$]$_n$ (**1**) from 10 to 273 K to determine whether intermetallic communication was evident. The data, corrected for the diamagnetic contributions of the ligands,[13] was fit to $\chi = C/(T - \theta) + \chi_o$, which revealed that **1** is best considered a simple paramagnet ($\mu_{eff} = 2.67\ \mu_B$, $C = 0.89$, $\theta = -0.86$, $\chi_o = -0.001$ emu/mol). The negative θ value—potentially indicative of weak antiferromagnetism—is too small to merit serious consideration, and the deviation from a spin-only value of 2.83 μ_B is common for V^{3+} complexes.[13,14] A lower moment may be associated with a reduced spin−orbit

(11) Mecozzi, S.; West, A. P.; Dougherty, D. A. *Proc. Natl. Acad. Sci. U.S.A.* **1996**, *93*, 10566−10571.
(12) (a) Klebe, G.; Diederich, F. *Philos. Trans. R. Soc. London, A* **1993**, *345*, 37−48. (b) Bacon, G. E.; Curry, N. A.; Wilson, S. A. *Proc. R. Soc. London, A* **1964**, *279*, 98−110.
(13) Carlin, R. L. *Magnetochemistry*; Springer-Verlag: Berlin, 1986.

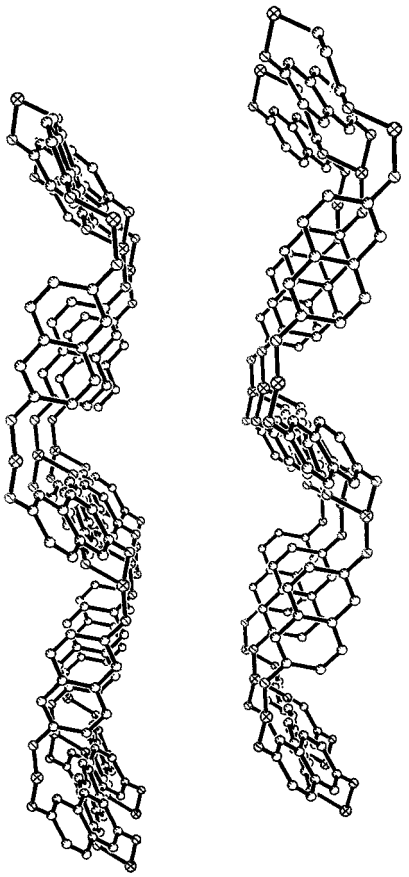

Figure 3. Layers of [*mer*-V($\mu_{2,6}$-$OC_{10}H_6O$)$_{1.5}$(4-(3-phenylpropyl)py)$_3$]$_n$ (**1**) revealing the boatlike rings that comprise the bricks (4-(3-phenylpropyl)pyridines removed).

coupling constant evident in complexes possessing a significant degree of covalency, as in the triaryloxide vanadium(III) compound **1**.

2-Dimensional [*mer*-V($\mu_{2,6}$-$OC_{10}H_6O$)$_{1.5}$(4-(3-phenylpropyl)-py)$_3$]$_n$ (**1**) has channels that are roughly 12 × 20 Å in size that might permit an exchange of ligands at the V(III) center. Attempts to substitute the 4-(3-phenylpropyl)pyridines with small molecules such as 2-butyne, trimethylphosphine, and diphenylacetylene failed despite observation by ^{1}H NMR spectroscopy that some loss of pyridine was incurred. Treatment of **1** with the oxygen atom source pyridine *N*-oxide in benzene for 2−3 h at 85 °C resulted in the formation of a black material whose crystals retained their original morphology. Upon examination by powder XRD, the material proved to be amorphous, and degradation in CD_3OD revealed the presence of bis-2,6-dinaphthol and pyridine in addition to the ligands, according to ^{1}H NMR spectra.

1-Dimensional [($\mu_{2,6}$-$OC_{10}H_6O$)(4-(3-phenylpropyl)py)$_2$VO]$_n$ (2). 1. Synthesis. Since aspects of the oxidation of **1** appeared intriguing, an attempt was made to generate oxo derivatives directly. Treatment of (^{i}PrO)$_3$VO with excess 2,6-dihydroxynaphthalene in 4-(3-phenylpropyl)pyridine at 100 °C afforded dark orange crystals of [($\mu_{2,6}$-$OC_{10}H_6O$)(4-(3-phenylpropyl)py)$_2$-VO]$_n$ (**2**) within 1−4 d (eq 3). Examination of the filtrate from

$$(^i\mathrm{PrO})_3\mathrm{VO} + 2\mathrm{HOC_{10}H_6OH} \xrightarrow[100\ ^\circ\mathrm{C}]{\text{4-(3-phenylpropyl)py}} 3\,^i\mathrm{PrOH} + 0.5(2,6\text{-}(\mathrm{HO})_2\mathrm{C_{10}H_5})_2 + [(\mu_{2,6}\text{-}\mathrm{OC_{10}H_6O})(\text{4-(3-phenylpropyl)py})_2\mathrm{VO}]_n\ (\mathbf{2}) \quad (3)$$

this reaction revealed the presence of bis-2,6-dinaphthol, which was identified via ^{1}H NMR spectroscopy via comparison to an authentic sample.

Table 3. Selected Interatomic Distances (Å) and Angles (deg) in [($\mu_{2,6}$-$OC_{10}H_6O$)(4-(3-phenylpropyl)py)$_2$VO]$_n$ (**2**)

V−O1	1.605(3)	V−N1	2.125(4)	O2−C1	1.347(4)
V−O2	1.883(3)	V−N2	2.136(3)	O3−C6	1.365(5)
V−O3	1.872(3)				
O1−V−O2	120.3(2)	N1−V−O1	96.3(2)	N2−V−O2	88.2(1)
O1−V−O3	119.1(2)	N1−V−O2	85.9(1)	N2−V−O3	85.4(1)
O2−V−O3	120.6(1)	N1−V−O3	88.1(1)	V−O2−C1	135.6(3)
N1−V−N2	167.5(4)	N2−V−O1	96.1(2)	V−O3−C6	133.0(3)

2. X-ray Crystal Structure. Details of the data collection and refinement are provided in Table 1, and pertinent geometric parameters of the 1-dimensional chain ($\mu_{2,6}$-$OC_{10}H_6O$)(4-(3-phenylpropyl)py)$_2$VO]$_n$ (**2**) are given in Table 3. A powder pattern calculated using the single-crystal data matched that of the bulk material.

The geometry about the vanadium is almost perfectly trigonal bipyramidal, with the oxo and the two aryloxides occupying equatorial positions ($\angle$(O−V−O) = 120.0(8)°$_{av}$) and the two 4-(3-phenylpropyl)pyridines residing in axial sites ($\angle$(N−V−N) = 167.5(4)°). The vanadium−oxo bond length of 1.605(3) Å,[15] the vanadium−aryloxide bond distances of 1.872(3) and 1.883(3) Å, and the 2.125(4) and 2.136(3) Å pyridine interactions are normal for a V(IV) species. The oxo group exerts a subtle influence on the 4-(3-phenylpropyl)pyridines, which is reflected in O_{oxo}−V−N angles (96.3(2)°, 96.1(2)°) that are significantly greater than the corresponding O_{OAr}−V−N angles (86.9(15)°$_{av}$).

As Figure 4 illustrates, the equatorial plane is virtually coincident with the direction of the chain, and each oxo is aligned perpendicular to the chain vector. The axial 4-(3-phenylpropyl)pyridines also extend perpendicular to the chain, but the conformations of the $(CH_2)_3$ groups orient to permit the phenyl ring to interact with the pyridine ring of an adjacent ligand (centroid to centroid d = 5.15 Å). Inspection of this close contact reveals that the closest approach is edge−edge, perhaps reflecting the different charge distribution of the N-substituted py ring versus a regular phenyl.[11] In subtle contrast, two interchain pyridine ring-edge to phenyl-face interactions ((centroid to centroid d = 4.61 and 5.14 Å)[12] are responsible for a tight packing of the chains, resulting in a sheet of similarly disposed oxo ligands. Naturally, the next layer to the oxo side has its oxo ligands aligned in opposition, such that adjacent sheets form a sandwich structure with the oxos oriented to the inside, and no net dipole is present. No significant (<5.5 Å) intersheet π-stacking or aromatic edge to face interactions have been detected.

1-Dimensional [($\mu_{1,4}$-OC_6H_4O)(py)$_2$VO]$_n$ (3). 1. Synthesis. Another 1-dimensional chain was prepared by heating (^{i}PrO)$_4$V and hydroquinone in pyridine under conditions (100 °C, 7 d) nominally used to prepare [*trans*-V($\mu_{1,4}$-OC_6H_4O)$_2$py$_2$·py]$_n$.[4] A small amount of [($\mu_{1,4}$-OC_6H_4O)(py)$_2$VO]$_n$ (**3**) was isolated from the reaction, and the quantity suggested that the oxo derived from water, perhaps via insufficient drying of the hydroquinone. When wet 1,4-HOC_6H_4OH was employed in the reaction to ensure the presence of a stoichiometric amount of H_2O, [($\mu_{1,4}$-OC_6H_4O)(py)$_2$VO]$_n$ (**3**) was prepared essentially quantitatively according to eq 4.

(14) Cotton, F. A.; Wilkinson, G. *Advanced Inorganic Chemistry*, 4th ed.; John Wiley & Sons: New York, 1972.
(15) Nugent, W. A.; Mayer, J. M. *Metal−Ligand Multiple Bonds*; Wiley-Interscience: New York, 1988.

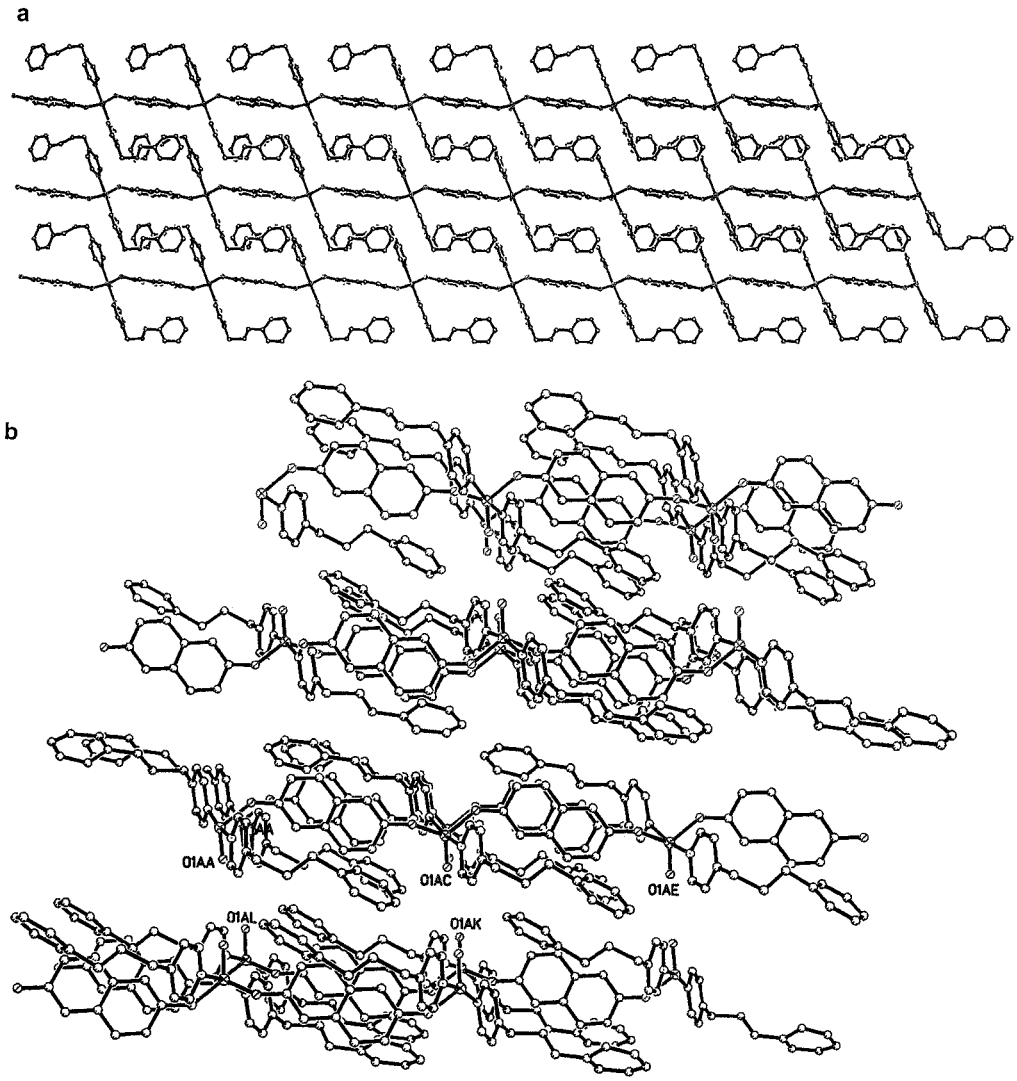

Figure 4. 1-Dimensional chain of $[(\mu_{2,6}\text{-}OC_{10}H_6O)(4\text{-}(3\text{-phenylpropyl})py)_2VO]_n$ (**2**) (a) and sheets (b) of **2** whose vanadyl orientations alternate.

$$(^{i}PrO)_4V + HOC_6H_4OH + H_2O \xrightarrow[2-7\ d]{py,\ 100\ ^\circ C} 4\,^{i}PrOH + [(\mu_{1,4}\text{-}OC_6H_4O)(py)_2VO]_n\ (\mathbf{3}) \quad (4)$$

2. X-ray Crystal Structure. Table 1 lists the pertinent details of the X-ray structure determination of $[(\mu_{1,4}\text{-}OC_6H_4O)(py)_2VO]_n$ (**3**). The powder pattern calculated from the single-crystal data proved to match the bulk yellow crystalline material. The core geometry of **3** is virtually identical to that of $[(\mu_{2,6}\text{-}OC_{10}H_6O)(4\text{-}(3\text{-phenylpropyl})py)_2VO]_n$ (**2**), and selected bond distances and angles are given in Table 4.

As in 2, the equatorial plane of $[(\mu_{1,4}\text{-}OC_6H_4O)(py)_2VO]_n$ (**3**) is almost coincident with the direction of the infinite chain, and all of the oxos are aligned and oriented essentially perpendicular to the chain (Figure 5). The pyridines of adjacent chains interpenetrate, but this does not appear to be a favorable π-stacking interaction since the rings are offset in a configuration that should not maximize electrostatic attractions,[11] even though the ring centroid to centroid distance is 4.41 Å. It is likely that the sheets comprised of chains of alternating oxo orientations are formed due to simple packing requirements to minimize density. No significant intersheet interactions were detected.

Discussion

In an effort to generate V(IV) CMONs with significant intermetallic spacing, 2,6-dihydroxynaphthalene was used as a precursor to a $\mu_{2,6}\text{-}OC_{10}H_6O$ linkage, but formation of a V(IV) network proved to be significantly slower than oxidative coupling of the organic. Consequently, the 2-dimensional V(III) $[mer\text{-}V(\mu_{2,6}\text{-}OC_{10}H_6O)_{1.5}(4\text{-}(3\text{-phenylpropyl})py)_3]_n$ (**1**) compound formed, and the solvent employed, 4-(3-propylphenyl)-pyridine, proved to be crucial in filling channels in the material and buttressing the layers. It was disappointing that magnetic measurements indicated no intermetallic communication, but this observation was somewhat expected given the lack of magnetic interactions in the sheet compound, $[trans\text{-}V(\mu_{1,4}\text{-}OC_6H_4O)_2py_2\cdot py]_n$. In concert with band structure calculations conducted on $[trans\text{-}Ti(\mu_{1,4}\text{-}OC_6H_4O)_2py_2\cdot py]_n$ and related derivatives,[16] it appears that the mismatch in orbital energetics between the dioxyaromatic spacers and early transition metals may be difficult to overcome; hence, properties based on communication between metals are unlikely to be found. The use of later metals, lower valent metal species, and sulfur-containing organic linking agents may improve this situation. For now, applications of the current class of CMONs must focus on physical properties that do not rely on intermetallic interactions, and chemical (e.g., catalytic) properties.

Utilization of dihydroxynaphthalene with $(^{i}PrO)_3VO$ again afforded a reduced vanadium product, the coordination polymer $[(\mu_{2,6}\text{-}OC_{10}H_6O)(4\text{-}(3\text{-phenylpropyl})py)_2VO]_n$ (**2**). While there

(16) Merschrod, E. Ph.D. Thesis, Cornell University, Ithaca, NY, 1999.

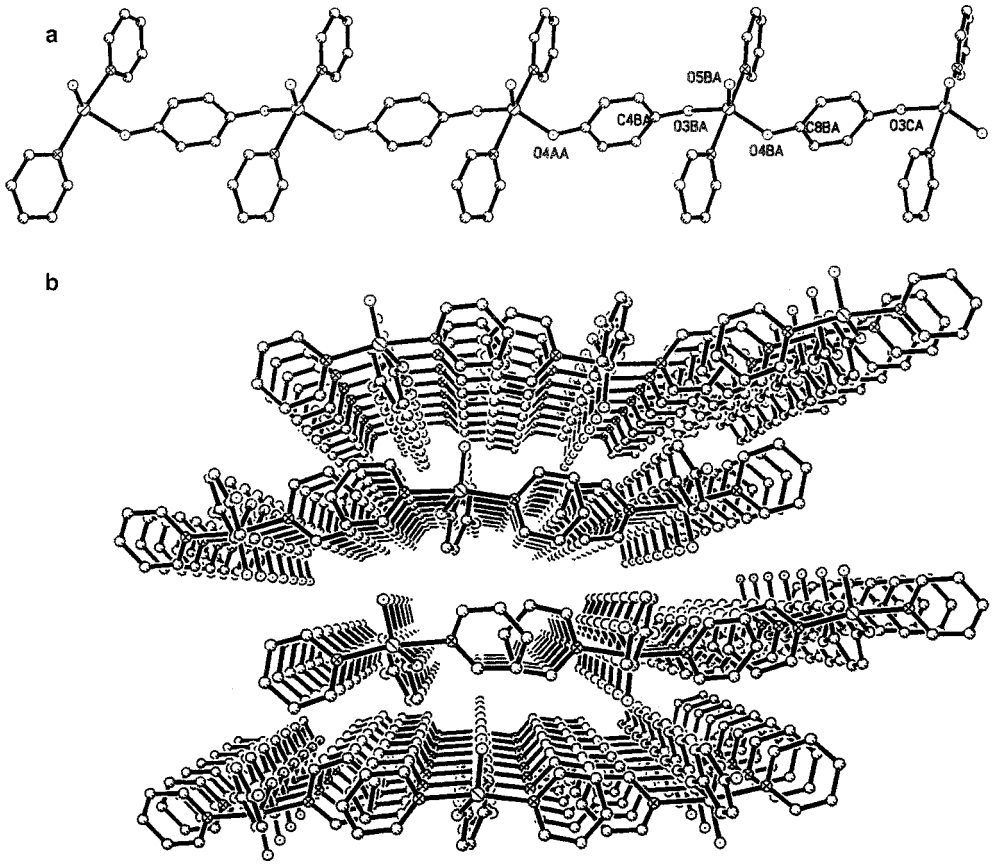

Figure 5. 1-Dimensional chain of $[(\mu_{1,4}\text{-}OC_6H_4O)(py)_2VO]_n$ (**2**) (a) and chains of alternate vanadyl orientations that form sheets (b).

Table 4. Selected Interatomic Distances (Å) and Angles (deg) in $[(\mu_{1,4}\text{-}OC_6H_4O)(py)_2VO]_n$ (**3**)

V−O5	1.599(6)	V−N1	2.13(1)	O3−C4	1.38(1)
V−O3	1.886(7)	V−N2	2.148(9)	O4−C8	1.34(1)
V−O4	1.877(8)				
O3−V−O4	119.9(3)	N1−V−O3	87.9(3)	N2−V−O4	89.2(4)
O3−V−O5	119.5(3)	N1−V−O4	86.6(4)	N2−V−O5	94.9(5)
O4−V−O5	120.6(3)	N1−V−O5	95.1(5)	V−O3−C4	129.9(7)
N1−V−N2	170.0(7)	N2−V−O3	86.3(3)	V−O4−C8	134.0(8)

are no bonding connections between strands, interchain interactions—primarily via the 4-(3-propylphenyl)pyridine ligand—produce a sheet structure. Edge to face pyridine−phenyl contacts, working in concert with related intramolecular packing forces that afford an appropriate conformation, provide enough attractive force to overcome potentially difficult dipole interactions of the highly polar VO^{2+} groups. Although each sheet has its oxo units oriented in one direction normal to the layer, no net dipole is evident in the complex because adjacent sheets have an opposite orientation. It is likely that the cancellation of dipoles is responsible for this type of packing, because no obvious interligand interactions are observed between sheets. With the simpler pyridine ligand present in 1-dimensional $[(\mu_{1,4}\text{-}OC_6H_4O)(py)_2VO]_n$ (**3**), no unusual interchain interactions are apparent, and adjacent strands exhibit vanadyl orientations that oppose one another. Despite these observations, the possibility of generating materials containing like-oriented vanadyl or related oxo groups is still enticing, especially if intersheet interactions can be designed into CMONs to encourage dipole alignment.[6]

Experimental Section

General Considerations. All manipulations were performed on a high-vacuum line or in an inert atmosphere drybox unless otherwise noted. Tetrahydrofuran was distilled from purple sodium benzophenone ketyl and then vacuum-transferred from the same into a glass bomb immediately prior to use in the drybox. Pyridine was refluxed over sodium, vacuum-transferred onto activated 4 Å molecular sieves, and vacuum-transferred into a glass bomb for storage in the drybox. Hydroquinone (Aldrich, 99+%) and 2,6-dihydroxynaphthalene (Aldrich, 98%) were dried by being dissolved in dry THF and removing the volatiles; this procedure was repeated three times. $(^iPrO)_3VO$ (Strem Chemicals, 98+%) and 4-(3-phenylpropyl)pyridine (Aldrich, 97%) were used as received and stored in the drybox. $(^iPrO)_4V$ was prepared by the literature method.[8] DCl (20 wt % in D_2O, Aldrich), D_2O (Cambridge Isotope Laboratories, 99.9% D), and CD_3OD (Cambridge Isotope Laboratories, 99.8% D) were used as received; solutions for ^1H NMR spectra were ca. 3 wt % DCl (∼1 M) and were prepared on the benchtop.

^1H NMR spectra were obtained on Varian XL-200 and VXR 400S spectrometers. Powder diffraction was performed on a Scintag XRD system-interfaced PC with Windows NT. Standard powder patterns were recorded as continuous scans with a chopper increment of $2\theta = 0.03°$ and a scan rate of 2 deg/min. Magnetic measurements of $[mer\text{-}V(\mu_{2,6}\text{-}OC_{10}H_6O)_{1.5}(4\text{-}(3\text{-phenylpropyl})py)_3]_n$ (**1**) were performed on a Quantum Design MPMS SQUID magnetometer operating at 0.5 T from 10 to 273 K.

Procedures. 1.a. Preparation of $[mer\text{-}V(\mu_{2,6}\text{-}OC_{10}H_6O)_{1.5}(4\text{-}(3\text{-phenylpropyl})py)_3]_n$ (1). $(^iPrO)_4V$ (200 mg, 0.70 mmol) and 2,6-dihydroxynaphthalene (334 mg, 2.08 mmol) were combined in a 10 mm o.d. glass tube along with ∼2 mL of 4-(3-phenylpropyl)pyridine. An immediate black coloration resulted, and the tube was sealed under vacuum and heated at 100 °C. Very small crystals were observed after a few days, and the product was collected after 35 d, washed with THF to remove excess 2,6-dihydroxynaphthalene and bis-2,6-dinaphthol, and dried by vacuum for >20 min. ^1H NMR spectra of **1** degraded in CD_3OD/DCl indicated a $DOC_{10}H_6OD$:4-(3-phenylpropyl)pyridine ratio of 1.5:2.25−3, depending on how thoroughly the sample had been washed with THF. Anal. Calcd for $C_{57}H_{54}O_3N_3V$ (found): C, 77.78 (77.54); H, 6.14 (5.90); N, 4.77 (4.63). IR (Nujol, cm^{-1}): 1620(m),

1581(s), 1236(s), 1144(m), 1108(m), 1065(w), 1026(w), 972(w), 964(w), 947(m), 838(w), 798(w), 768(w), 740(s), 701(m), 667(w), 527(m), 601(w), 576(w), 527(w), 489(w), 471(w).

1.b. Identification of Byproduct [2,6-(HO)$_2$-C$_{10}$H$_6$]$_2$. The filtrate from a typical preparation of **1** was used to verify the coupled 2,6-dihydroxynaphthalene oxidation product. The filtrate was quenched with 1 M HCl, and THF was removed in vacuo. The organic components were extracted into ethyl acetate, dried over anhydrous $MgSO_4$, and concentrated. A very slightly soluble light pink solid was filtered away. Flash chromatography (silica gel) of the remaining material with hexanes/ethyl acetate (70:30) permitted separation of excess 2,6-dihydroxynaphthalene. A second procedure using a 60:40 hexanes/ethyl acetate mixture allowed separation of byproduct bis-2,6-dinaphthol ((2,6-(HO)$_2$C$_{10}$H$_6$)$_2$; $R_f = 0.07$).

2. Preparation of Bis-2,6-dinaphthol. 2,6-Dihydroxynaphthalene (1.8 g, 11.0 mmol) was dissolved in CH_3CN and treated with ferric chloride hexahydrate (2.977 g, 11.0 mmol) dissolved in water. The mixture was stirred at room temperature for 1.5 h under Ar, at which time the solution was a dark pink color. The acetonitrile was removed in vacuo to give some white precipitate. The organics were extracted into ethyl acetate, washed with NaCl(satd), and dried over $MgSO_4$. The solution was reduced on a rotary evaporator, and a small amount of insoluble pink solid was filtered before the volume was reduced further for introduction onto a silica gel column. A 60:40 EtOAc/hexanes mixture was used to separate the coupled product ($R_f = 0.07$) from remaining starting material (which came off the column first) and oligomeric byproducts. Only ~5% yield was obtained due to the gentle conditions and short reaction time used. ^{1}H NMR (acetone-d_6): δ 6.87 (dd, $J = 9.2$, 2.4 Hz, 2H), 6.93 (d, $J = 8.8$ Hz, 2H), 7.21 (d, $J = 2.4$ Hz, 2H), 7.24 (d, $J = 8.8$ Hz, 2H), 7.50 (br s, 2H), 7.69 (d, $J = 8.8$ Hz, 2H), 8.31 (br s, 2H). ^{13}C{^{1}H} NMR (acetone-d_6): δ 110.45 (CH), 115.33 (binaphthyl C), 119.26 (CH), 119.83 (CH), 127.17 (CH), 128.75 (CH), 130.06 (naphthalene C), 131.25 (naphthalene C), 152.25 (COH), 154.08 (COH). Anal. Calcd for $C_{20}H_{14}O_4$ (found): C, 75.46 (73.59); H, 4.43 (4.73); N, 0.00 (<0.02).

3. Preparation of [($\mu_{2,6}$-OC$_{10}$H$_6$O)(4-(3-phenylpropyl)py)$_2$VO]$_n$ (2). (^{i}PrO)$_3$VO (150 mg, 0.62 mmol) and 2,6-dihydroxynaphthalene (396 mg, 2.48 mmol) were combined in a 10 mm o.d. glass tube along with ~4 mL of 4-(3-phenylpropyl)pyridine. An brown-colored solution resulted immediately in addition to a solid black mass. The tube was sealed under vacuum and heated at 100 °C. Crystals were observed after 24 h, and the product was collected after 4 d, washed with THF, and dried by vacuum for >20 min. Inspection of a sample in Paratone oil under a microscope revealed orange crystals. Powder XRD matched the theoretical pattern calculated from the single-crystal data. ^{1}H NMR of a typical sample degraded in CD_3OD/DCl indicated a DOC$_{10}$H$_6$-OD:4-(3-phenylpropyl)pyridine ratio of 1:1.42, slightly less than expected from the single-crystal stoichiometry. Analysis of the fitrate similar to that described in section 1.b. revealed the presence of bis-2,6-dinaphthol. Anal. Calcd for $C_{38}H_{36}O_3N_2V$ (found): C, 73.65 (73.42); H, 5.81 (5.67); N, 4.52 (4.45). IR (Nujol, cm^{-1}): 1620(m), 1584(s), 1233(s), 1178(w), 1144(m), 1110(m), 1067(w), 1026(w), 971(w), 965(w), 948(m), 881(w), 862(w), 838(w), 770(w), 742(s), 700(w), 635(m), 604(w), 575(w), 529(w), 489(w), 470(w).

4. Preparation of [($\mu_{1,4}$-OC$_6$H$_4$O)(py)$_2$VO]$_n$ (3). (^{i}PrO)$_4$V (90 mg, 0.31 mmol) and undried hydroquinone (178 mg, 1.57 mmol; HOC$_6$H$_4$-OH·0.2 H$_2$O by ^{1}H NMR spectroscopic analysis in dry acetone-d_6) along with dried hydroquinone (690 mg, 6.3 mmol) were combined in a 10 mm o.d. glass tube along with ~3 mL of pyridine. A yellow-colored solution resulted immediately in addition to a solid black mass. The tube was sealed under vacuum and heated at 100 °C. Crystals were observed after a few days, and the product was collected after 1 week, washed with THF, and dried under vacuum for >20 min. Inspection of a sample in Paratone oil under a microscope revealed yellow crystals. Powder XRD matched the theoretical pattern calculated from the single-crystal data. A ^{1}H NMR spectrum of a sample degraded in D_2O/DCl indicated a DOC$_6$H$_4$OD:pyridine ratio of ~1:1.3, less than expected from the single-crystal stoichiometry. Anal. Calcd for $C_{16}H_{14}O_3N_2V$ (found): C, 57.62 (60.71); H, 4.20 (4.47); N, 8.40 (7.79). IR (Nujol, cm^{-1}): 1602(w), 1555(w), 1245(s), 1229(s), 1066(w), 1042(w), 1012-(w), 972(w), 827(s), 694(w), 639(w), 500(w), 457(m).

Single-Crystal X-ray Structure Determinations. 5. X-ray Structure Determination of [V($\mu_{2,6}$-OC$_{10}$H$_6$O)$_{1.5}$(4-(3-phenylpropyl)py)$_2$]$_n$ (1). Crystals of **1** were grown from 4-(3-phenylpropyl)pyridine as described above. A few milligrams of the orange chips were suspended in Paratone oil on a glass slide. Handling the crystals in Paratone for a few hours in the ambient atmosphere caused only minor decomposition, but the material turned completely black after 2 d. Under a microscope, a single orange-yellow plate crystal (0.065 × 0.050 × 0.020 mm) was isolated in a rayon fiber loop epoxied to a glass fiber.[17,18] On the F2 line at CHESS ($\lambda = 0.9808$ Å), the crystal was frozen in a 110 K nitrogen stream. Using a 0.2 mm collimator, a Quantum 4 CCD was employed to record diffraction with a crystal to detector distance of 60 mm.[19] Data were collected as 90 s, 15° oscillations in ϕ, with a total of 360° collected, yielding 10 032 reflections. The first frame was indexed to a *P* triclinic unit cell using the program DENZO,[20] as were the subsequent frames, and all the data were scaled together with SCALEPACK (3110 unique reflections ($R_{int} = 0.0413$); the numbers of data/restraints/parameters were 110/0/613). Observed intensities were corrected for Lorentz and polarization effects, and no absorption correction was applied. The structure solution was obtained by direct methods (SHELXTL) in *P*1, and after some initial refinement was transferred into $P\bar{1}$. Hydrogen atoms were introduced geometrically, and disorder in one of the phenylpropyl moieties was modeled. The structure was refined by full-matrix least-squares on F^2 using anisotropic thermal parameters for all non-hydrogen atoms.

6. X-ray Structure Determination of [($\mu_{2,6}$-OC$_{10}$H$_6$O)(4-(3-phenylpropyl)py)$_2$VO]$_n$ (2). Crystals large enough for structure determination were grown from 4-(3-phenylpropyl)pyridine as explained above. A few milligrams of crystals were suspended in Paratone oil on a glass slide. Under a microscope, a single dark orange block (0.50 × 0.18 × 0.16 mm) was isolated in a rayon fiber loop epoxied to a metal fiber. X-ray diffraction data were collected on a Siemens SMART system ($\lambda = 0.710\,69$) employing a 1K CCD detector and an Oxford Cryostream set at 173 K. Observed intensities were corrected for Lorentz and polarization effects, and a semiempirical absorption correction was applied (SADABS). The reflections collected totaled 18 290, with 6963 ($R_{int} = 0.0651$) unique (the numbers of data/restraints/parameters were 5402/0/449). The structure was solved by direct methods (SHELXTL). One 4-(3-phenylpropyl)pyridine per vanadium exhibited disorder of the phenylpropyl moiety, having two equally probable orientations. The occupancy was refined while the thermal parameters were restrained and vice versa. Hydrogen atoms were added geometrically. The structure was refined by full-matrix least-squares on F^2 using isotropic thermal parameters for all non-hydrogen atoms.

7. X-ray Structure Determination of [($\mu_{1,4}$OC$_6$H$_4$O)(py)$_2$VO]$_n$ (3). Crystals large enough for structure determination were grown from pyridine as explained above. A few milligrams of crystals were suspended in Paratone oil on a glass slide. Under a microscope, a single yellow needle (0.140 × 0.050 × 0.020 mm) was picked up in a 100 μm rayon fiber loop epoxied to a metal fiber. X-ray diffraction data were collected on a Siemens SMART system ($\lambda = 0.710\,69$) employing a 1K CCD detector and an Oxford Cryostream set at 165 K. Observed intensities were corrected for Lorentz and polarization effects, and a semiempirical absorption correction was applied (SADABS). The reflections collected totaled 4129, with 1924 ($R_{int} = 0.1238$) unique (the numbers of data/restraints/parameters were 875/0/255). The structure was solved by direct methods (SHELXTL). Hydrogen atoms were located in the difference Fourier map and included in the model.

(17) Blond, L.; Pares, S.; Kahn, R. *J. Appl. Crystallogr.* **1995**, *28*, 653−654.
(18) A thorough explanation of the construction of fiber loops and experimental methods at CHESS is given in Walter, R. L. Ph.D. Thesis, Cornell University, Ithaca, NY, 1996.
(19) (a) Thiel, D. J.; Walter, R. L.; Ealick, S. E.; Bilderback, D. H.; Tate, M. W.; Gruner, S. M.; Eikenberry, E. F. *Rev. Sci. Instrum.* **1995**, *3*, 835−844. (b) Walter, R. L.; Thiel, D. J.; Barna, S. L.; Tate, M. W.; Wall, M. E.; Eikenberry, E. F.; Gruner, S. M.; Ealick, S. E. *Structure* **1995**, *3*, 835−844.
(20) Otwinski, Z. DENZO, a program for automatic evaluation of film densities, Department for Molecular Biophysics and Biochemistry, Yale University, New Haven, CT, 1988.

The structure was refined by full-matrix least-squares on F^2 using isotropic thermal parameters for all non-hydrogen atoms.

Acknowledgment. We thank John M. Pette and Emil B. Lobkovsky for experimental assistance and Prof. Yuri Suzuki for use of the SQUID magnetometer. We gratefully acknowledge contributions from the National Science Foundation (Grant CHE-9816134), CHESS, the Cornell Center for Materials Research (Grant DMR-9632275; CCMR REU to J.P.), and Cornell University.

Supporting Information Available: X-ray structural data pertaining to [*mer*-V($\mu_{2,6}$-$OC_{10}H_6O)_{1.5}$(4-(3-phenylpropyl)py)$_3$]$_n$ (**1**), [($\mu_{2,6}$-$OC_{10}H_6O$)(4-(3-phenylpropyl)py)$_2$VO]$_n$ (**2**), and [($\mu_{1,4}$-OC_6H_4O)(py)$_2$-VO]$_n$ (**3**): a summary of crystallographic parameters, atomic coordinates, bond distances and angles, and anisotropic thermal parameters. This material is available free of charge via the Internet at http://pubs.acs.org.

IC000756Z